High Capacity, Charge-Selective Protein Uptake by Polyelectrolyte Brushes

Andy Kusumo,[†] Lindsay Bombalski,[‡] Qiao Lin,[§] Krzysztof Matyjaszewski,[‡] James W. Schneider,[†] and Robert D. Tilton*[,†,||]

Department of Chemical Engineering, Department of Chemistry, and Department of Biomedical Engineering, Carnegie Mellon University, Pittsburgh, Pennsylvania 15213 and Department of Mechanical Engineering, Columbia University, New York, New York 10027

Received December 18, 2006. In Final Form: February 2, 2007

Surface plasmon resonance was used to measure binding of proteins from solution to poly(2-(dimethylamino)ethyl methacrylate) (PDMAEMA) brushes end-grafted from gold surfaces by atom transfer radical polymerization (ATRP). PDMAEMA brushes were prepared with a variety of grafting densities and degrees of polymerization. These brushes displayed charge selective protein uptake. The extent of uptake for net negatively charged bovine serum albumin (BSA) scaled linearly with the surface mass concentration of grafted PDMAEMA, regardless of grafting density. BSA was bound at a constant ratio of 120 DMAEMA monomer units per protein molecule for all brushes examined. The equivalent three-dimensional concentration of BSA bound in the brush (i.e., the bound BSA surface excess concentration divided by the brush thickness) decreased monotonically with decreasing grafting density. The concentration of BSA bound within brushes prepared at higher grafting densities was comparable with the aqueous protein solubility limit. BSA desorption from the brush required changes in solution pH and/or ionic strength to eliminate its net electrostatic attraction to PDMAEMA. Net positively charged lysozyme was completely rejected by the PDMAEMA brushes.

Introduction

Nonspecific adsorption of proteins to charged interfaces is the basis for ion exchange chromatography. Compared to other stationary-phase protein separation modes, ion-exchange chromatography has the advantage of preserving protein biological activity due to its mild elution conditions.[1] Several factors influence the protein binding capacity of ion exchange media, including the total accessible area for protein adsorption. One strategy to increase binding capacity is the "tentacle ion exchanger", originally developed in the early 1990s. This consisted of linear chains made of 5−50 charged repeat units grafted onto a porous solid support.[2,3] Compared to the conventional ion exchangers where the ionic groups were directly attached on the support matrix, these grafted chains increased the binding capacity by up to 300% with a simultaneous increase in the resolution of the protein separation. This configuration was also believed to minimize undesirable adsorption to the underlying support. Detailed descriptions of chain grafting densities or conformations are not available for these materials.

Systematic experimental studies of protein adsorption on well-defined, grafted polyelectrolyte layers are limited. Kato and co-workers studied protein adsorption on poly(ethylene terephthalate) (PET) fibers modified with different grafted polyelectrolytes.[4] They found at physiological pH acidic immunoglobulin G (aIgG) adsorbed more on anionic acrylic acid- and methacryloyloxyethyl phosphate-based grafted chains than on cationic dimethylaminoethyl methacrylate-based chains, whereas basic immunoglobulin G (bIgG) showed the opposite behavior. Protein adsorption on grafted layers was dominated by the net electrostatic interaction between the proteins and the charged grafts. A small amount of adsorption was observed when the protein and the graft carried the same net charge. It was not determined whether this was due to adsorption on the PET substrate or to some other interaction with the grafts. Sukhishvili and Granick[5] compared adsorption of negatively charged human serum albumin (HSA) on physisorbed layers and grafted layers of cationic poly-4-vinylpyridine (QPVP). They found that the graft layer had a higher internal binding capacity toward HSA, as well as greater preservation of HSA secondary structure, than the physisorbed layer. HSA washout from the graft layer was also hindered relative to the physisorbed layer. Tran and co-workers measured lysozyme and fibrinogen adsorption to anionic poly(styrene sulfonic acid) brushes.[6] These brushes adsorbed both net positively charged lysozyme and also net negatively charged fibrinogen. The authors argued that positive sites on the fibrinogen molecule were sufficiently well distributed to allow localized electrostatic attraction to charged polyelectrolyte segments. Neutron reflectivity measurements showed that the proteins were located on the periphery of the brush, with fibrinogen located further out than lysozyme. Recently, similar results were reported by Wittemann and co-workers[7] in which anionic poly(acrylic acid) adsorbed net negatively charged bovine serum albumin (BSA).

Here we report a systematic study of the extent and reversibility of charge-specific protein adsorption by cationic polyelectrolyte brushes as a function of the grafted chain contour length and grafting density. Poly(2-(dimethylamino)ethyl methacrylate) (PDMAEMA) brushes were grafted from gold surfaces using atom transfer radical polymerization (ATRP). Direct polymerization of a brush starting with a surface-bound initiator (i.e., grafting from) can produce higher grafting densities than are

* To whom correspondence should be addressed. E-mail tilton@andrew.cmu.edu.
[†] Department of Chemical Engineering, Carnegie Mellon University.
[‡] Department of Chemistry, Carnegie Mellon University.
[§] Columbia University.
[||] Department of Biomedical Engineering, Carnegie Mellon University.

(1) Staby, A.; Jensen, I. H. *J. Chromatogr. A* **2001**, *908*, 149−161.
(2) Müller, W. *J. Chromatogr. A* **1990**, *510*, 133−140.
(3) Donovan, J.; Rabel, F.; Zahran, J. *Am. Biotechnol. Lab.* **1991**, *9*, 20−22.
(4) Kato, K.; Sano, S.; Ikada, Y. *Colloids Surf. B* **1995**, *4*, 221−230.
(5) Sukhishvili, S. A.; Granick, S. *J. Chem. Phys.* **1999**, *110*, 10153−10161.
(6) Tran, Y.; Auroy, P.; Lee, L.-T.; Stamm, M. *Phys. Rev. E* **1999**, *60*, 6984−6990.
(7) Wittemann, A.; Haupt, B.; Ballauff, M. *Phys. Chem. Chem. Phys.* **2003**, *5*, 1671−1677.

10.1021/la063660b CCC: $37.00
Published on Web 03/15/2007

Table 1. BSA Adsorption to Grafted PDMAEMA Layers at 0.1 mg/mL in 1 mM NaCl

ID	M_n (g/mol)	$\Gamma_{PDMAEMA}$ (mg/m^2)	σ^{-1} (nm^2)[a]	$2R_g\sigma^{1/2}$	Γ_{BSA} (mg/m^2)	n_{DMAEMA}/n_{BSA}	H (nm)	$C_{3D,BSA}$ (mg/mL)
1	12 000	6.9	3	2.6	24.1	120	19	1274
2	12 000	9.4	2	3.0	35.9	110	19	1897
3	47 000	11	7	3.3	36.3	127	74	490
4	80 000	13.6	10	3.7	53.7	106	126	426
5	100 000	3.1	54	1.7	10.7	122	158	68
6	100 000	3.8	44	1.9	9.2	174	158	58
7	100 000	4.4	38	2.1	28.3	65	158	179
8	100 000	5.1	33	2.2	16.3	132	158	103

[a] Surface area per PDMAEMA chain σ^{-1} calculated from M_n and $\Gamma_{PDMAEMA}$.

achievable by grafting a pre-existing polymer to a surface. Thus, it is possible to create a broader range of polyelectrolyte layer configurations than other polymer grafting strategies. Surface plasmon resonance (SPR) measurements indicated that cationic PDMAEMA brushes display an extremely high binding capacity for net negatively charged BSA, while completely rejecting net positively charged lysozyme proteins. The extent of BSA uptake in the PDMAEMA brushes scaled linearly with the mass of PDMAEMA in the brush, independent of grafting density, strongly suggesting an imbibition of the protein into the interior of the PDMAEMA brush. The binding capacity of PDMAEMA brushes for BSA was comparable to the highest values reported in the ion exchange literature, namely the absorption of cytochrome *c* into anionic polyacrylamide-based hydrogels as reported by Lewus and Carta.[8] We also identify conditions that are suitable for desorbing BSA from the brush, a requirement for the eventual application of such materials as ion exchange media for protein separations.

Experimental Section

Materials. 2-(Dimethylamino)ethyl methacrylate (Aldrich, 99%) was purified by passage through a basic alumina column to remove the stabilizer. CuBr (Aldrich, 99.999%) was purified by washing sequentially with acetic acid and diethyl ether, filtration, and drying and was stored under nitrogen before use. Pure ethanol (Pharmco Products Inc), $CuBr_2$ (Aldrich, 99.999%), *N*,*N*,*N*′,*N*″,*N*‴,*N*⁗-hexamethyltriethylenetetramine (HMTETA) (Aldrich, 99%), acetone (HPLC grade, Aldrich), methylene chloride (HPLC grade, Fisher), tetrahydrofuran (HPLC grade, Aldrich), and sodium chloride (Acros, 99%) were used as received. Bis(2-hydroxy-ethyl)disulfide bis(2-bromopropionate) ($BHEDS(BP)_2$) was synthesized by procedures previously reported.[9]

Bovine serum albumin (A0281, >99%) and chicken egg lysozyme (L7651, 95%) were purchased from Sigma-Aldrich. BSA and lysozyme were dissolved in a pre-filtered (0.2 μm membrane filter) 1 mM NaCl solution and dialyzed for ~12 h at 4 °C against 1 mM NaCl solution prior to use. All water was deionized by reverse osmosis followed by final purification to 18.2 MΩ·cm resistivity using the Barnstead Nanopure Diamond system. The protein concentration was 0.1 mg/mL in all adsorption experiments.

Preparation of Gold Substrates. Substrates for SPR experiments were prepared on LaSFN or N-LaSF9 glass slides (Schott Glass Technologies, Inc.). The slides were cleaned following procedures described by Meldum and co-workers[10] prior to evaporative deposition of thin gold films on Cr adhesion layers. The slides were sonicated first in ethanol for 10 min, then in water for 10 min, then in 2% Hellmanex cleaning solution (Hellma GmbH & Co. KG) for 30 min, and finally in ethanol for 10 min. Slides were copiously rinsed with purified water between each sonication step. Chromium of purity 99.9% from chromium-plated tungsten rods and gold of purity >99.9% were evaporated consecutively onto cleaned LaSFN9 or N-LaSF9 glass slides using a thermal evaporator (Denton DV-502A). Two nanometers of chromium followed by 45 nm of gold were deposited at a rate of 0.2−0.3 Å/s at pressures $<5 \times 10^{-6}$ Torr. To reuse slides, chromium and gold were stripped using gold etchant TFA for 1 min and then chromium etchant 1020 for 1 min prior to sonicating in 2% Hellmanex solution. Both etchants were purchased from Transene Company, Inc.

ATRP of PDMAEMA from Gold Films. The gold-coated SPR slide was mounted in the SPR flowcell (see below) prior to chemisorption of initiator. A 0.5 mM solution of the $BHEDS(BP)_2$ initiator in ethanol was injected into the flow cell, and chemisorption to gold was allowed to occur for at least 24 h. Nonadsorbed initiator was rinsed subsequently with 5 mL of ethanol (~70 times the flow cell volume). In experiments 3 and 4 (Table 1), butyl disulfide was co-injected as a "dummy" or noninitiating spacer molecule on the gold surface to manipulate the PDMAEMA grafting density (4:1 molar ratio to $BHEDS(BP)_2$). After surface functionalization, the slide was removed and blown dry with nitrogen. $BHEDS(BP)_2$ served as the surface-bound initiator, from which PDMAEMA was grown. To perform the air-free polymerization, the slide was mounted in a machined Teflon encasement that protected and positioned it upright in a reaction flask inside a glove box (N_2 atmosphere). Deoxygenated $CuBr_2$ (0.0318 g, 0.1422 mmol), HMTETA (0.21 g, 0.84 mmol), ethyl 2-bromoisobutyrate (26.1 μL, 0.177 mmol), and 2-(dimethylamino)ethyl methacrylate (64.2 g, 354 mmol) were added to the reaction flask.[11−14] To increase the solubility of the deactivator complex (CuBr2-HMTETA), solvent (acetone, 50 vol %) was added.[15] Free ethyl 2-bromoisobutyrate was added to the solution to initiate polymerization in solution, concurrently with the surface-initiated polymerization. Purified CuBr (0.1014 g, 0.708 mmol) was added last in succession to commence the polymerization. The reaction mixture was stirred at 35 °C for a predetermined amount of time (based on the target molecular weight). Thereafter, the slides were removed and sonicated sequentially in acetone, tetrahydrofuran, and methylene chloride before being blown dry. Reactions were quenched by exposure to air and rinsing with chloroform. PDMAEMA synthesized from the free initiator in the bulk was used for molecular weight determination as described below. The catalyst was removed from the solution by passing over alumina, and the free polymer in solution was precipitated by addition of hexanes. The precipitated polymer samples were dissolved in dimethylformamide (DMF) for molecular weight determination via size exclusion chromatography.

Polymer Characterization. The molecular weight of polymer grown in the solution phase was analyzed by size exclusion chromatography (SEC), performed with *N*,*N*-dimethylformamide as the mobile phase at 50 °C using a Waters 510 pump set to a flow rate of 1 mL/min, with three Styragel columns (Polymer Standard

(8) Lewus, R. K.; Carta, G. *Ind. Eng. Chem. Res.* **2001**, *40*, 1548−1558.
(9) Tsarevsky, N. V.; Matyjaszewski, K. *Macromolecules* **2002**, *35*, 9009−9014.
(10) Meldrum, F. C.; Flath, J.; Knoll, W. *Langmuir* **1997**, *13*, 2033−2049.
(11) Davis, K. A.; Charleux, B.; Matyjaszewski, K. *J. Polym. Sci., Part A: Polym. Chem.* **2000**, *38*, 2274−2283.
(12) Matyjaszewski, K.; Miller, P. J.; Shukla, N.; Immaraporn, B.; Gelman, A.; Luokala, B. B.; Siclovan, T. M.; Kickelbick, G.; Vallant, T.; Hoffmann, H.; Pakula, T. *Macromolecules* **1999**, *32*, 8716−8724.
(13) Matyjaszewski, K.; Xia, J. *Chem. Rev.* (*Washington, D.C.*) **2001**, *101*, 2921−2990.
(14) Zhang, X.; Matyjaszewski, K. *Macromolecules* **1999**, *32*, 1763−1766.
(15) Zhang, X.; Xia, J.; Matyjaszewski, K. *Macromolecules* **1998**, *31*, 5167−5169.

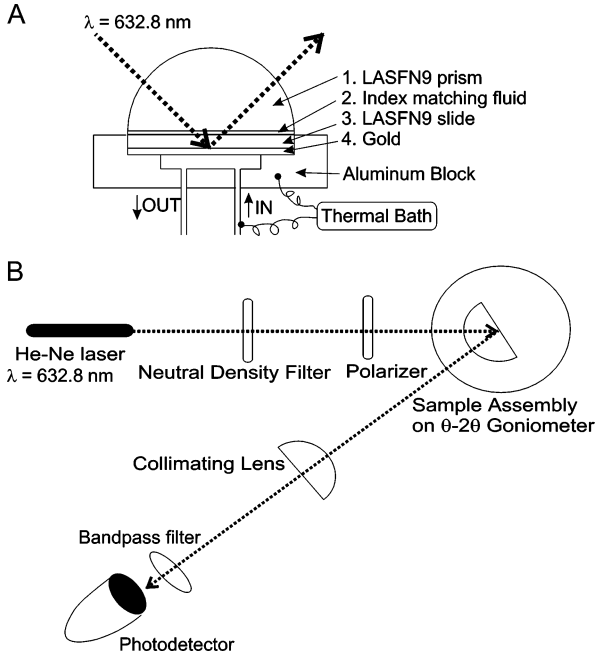

Figure 1. SPR instrument assembly based on the Kretschmann configuration. A. Laser incidence to the gold-coated slide. B. Optical path, supported on a θ-2θ goniometer. The incident beam is p-polarized.

Service, pore sizes 10^5, 10^3, and 10^2 Å), and a Waters 2410 refractive index detector. Molecular weights were determined using Polymer Standard Service (PSS) software with a calibration based on linear poly(methyl methacrylate) standards (from PSS). The measurement of polymer grown free in solution in parallel with surface-initiated ATRP was previously shown to provide an accurate representation of the surface-grafted polymer molecular weight.[16]

Surface Plasmon Resonance. SPR spectroscopy is highly sensitive to changes in the interfacial refractive index profile caused by thin films and adsorption and frequently has been used to quantify surface excess concentrations for a variety of surface active materials and surfaces.[17−20] The theory is described elsewhere by Knoll[21] and Hanken and co-workers.[22] We used SPR spectroscopy to measure the amount (mass per area) of PDMAEMA grafted from the gold surface and to measure the extent and kinetics of protein uptake in the grafted layers.

The SPR instrument was built in the Kretschmann configuration (Figure 1). An intensity-stabilized, linearly polarized He−Ne laser beam (λ = 632.8 nm, 1.5 mW, Melles Griot) passed through an absorptive OD1 neutral density filter (Newport) and a Glan-Thompson Calcite polarizer (Newport) to provide p-polarization at the solid/liquid interface and then through a LaSFN9 hemicylinder prism that was optically coupled to a LaSFN9 or N-LaSF9 slide by a high refractive index oil (Cargille Labs series B, n = 1.6911 at λ = 632.8 nm). The light reflected from the slide/solution interface was recollimated by a hemicylinder lens and passed through a bandpass filter to remove stray room light before striking a photodetector (International Light, Inc. Research Radiometer). Laser incident angles were driven on a θ-2θ goniometer by stepper motors that have 0.0025° resolution (Huber Diffraktionstechnik GmbH & Co. KG). To determine adsorbed amounts after adsorption had achieved steady-state, scans of reflectivity versus incident angle were recorded at 0.05° intervals.

The gold-coated slide served as one wall of an anodized aluminum fluid flow cell (oval-shaped with length, width, and depth of 1.5, 0.40, and 0.10 cm, respectively; total volume 73 μL), sealed with an inert Viton O-ring. The anodized aluminum block was maintained at 25 ± 0.1 °C by a high flow rate circulating water bath, calibrated against a NIST-calibrated thermometer (Fisherbrand). Solutions were incubated at 25 °C in the same water bath before being pumped through the cell using a peristaltic pump or simply injected by syringe.

The alignment of the SPR instrument was checked regularly by recording p-polarized reflectivity profiles for interfaces of clean LASFN9 (without the Cr/Au coating) with each of three standard fluids (air, water, ethanol). The angle at minimum reflectivity was required to fall within ±0.05° of the theoretically expected Brewster angle for each of the three interfaces.

Following Levchenko,[19] adsorption kinetics were monitored qualitatively by recording the reflectivity at a fixed angle of incidence where the reflectivity is most sensitive to adsorption. This angle was selected such that the absolute value of the slope of the theoretically predicted reflectivity vs incident angle ($dR/d\theta$) is maximized. The reflectivity, or reflection coefficient, is the intensity of the reflected beam normalized by the intensity of the incident beam. Full scans of reflectivity vs angle were recorded after the reflectivity was no longer changing. The suitability of SPR for quantifying adsorption was first verified by comparing the measured adsorption of BSA onto hydrophobic hexadecanethiol self-assembled monolayers, and the results were consistent with the literature for BSA adsorption on hydrophobic surfaces as discussed below.

To analyze SPR data, plots of reflectivity versus angle of incidence were regressed against the N-layer Fresnel model.[23] Each layer (glass, Cr, Au, polymer film, and ambient fluid) is assumed to be smooth and homogeneous and is parametrized by thickness and refractive index. The following indices of refraction[24−27] were used for data analysis: LaSFN9: n = 1.8449 (or N-LaSF9: n = 1.8449), Cr: n = 3.14 + 3.32i, aqueous solution (25 °C): n = 1.3319. Note that the refractive index mismatch between the high index matching fluid and the prism and slide has a negligible effect on the reflectivity profile in the measured angular range. Commercially available higher index fluids were avoided due to their toxicity and corrosiveness.

The thickness and refractive index of the gold-on-chromium film was determined prior to grafting the PDMAEMA layer. The bare-gold surface was immersed in 1 mM NaCl and angle-scanned at 25 °C, and the reflectivity profile was fitted to a four-layer model (N = 4) by χ^2 minimization. The adjustable parameters in the fitting were the thicknesses of the chromium film (d_{Cr}) and the gold film (d_{Au}), and the real (n_{Au}) and imaginary (k_{Au}) parts of the refractive index of the gold film. The real and imaginary parts of the refractive index of Cr were fixed. Gold film thickness results were consistent with the thickness recorded during the gold deposition using a quartz crystal microbalance in the evaporator.

Surface Concentration of Polymer and Protein. After grafting the PDMAEMA film, the slide was remounted in the SPR flowcell and equilibrated in 1 mM NaCl solution for 12 h at 25 °C. An angle scan was performed, and the measured reflectivity profile $R(\theta)$ was fitted with the five-layer model to determine the optical average refractive index n and thickness d of the polymer film, from which the surface concentration of the polymer Γ was determined as polymer

(16) Boyes, S. G.; Granville, A. M.; Baum, M.; Akgun, B.; Mirous, B. K.; Brittain, W. J. *Surf. Sci.* **2004**, *570*, 1−12.
(17) Sigal, G. B.; Mrksich, M.; Whitesides, G. M. *J. Am. Chem. Soc.* **1998**, *120*, 3464−3473.
(18) De Feijter, J. A.; Benjamins, J.; Veer, F. A. *Biopolymers* **1978**, *17*, 1759−1772.
(19) Levchenko, A. A.; Argo, B. P.; Vidu, R.; Talroze, R. V.; Stroeve, P. *Langmuir* **2002**, *18*, 8464−8471.
(20) Silin, V.; Weetall, H.; Vanderah, D. J. *J. Colloid Interface Sci.* **1997**, *185*, 94−103.
(21) Knoll, W. *Annu. Rev. Phys. Chem.* **1998**, *49*, 569−638.
(22) Hanken, D. G.; Jordan, C. E.; Frey, B. L.; Corn, R. M. *Electroanal. Chem.* **1998**, *20*, 141−225.
(23) Hansen, W. N. *J. Opt. Soc. Am.* **1968**, *58*, 380−390.
(24) Johnson, P. B.; Christy, R. W. *Phys. Rev. B* **1974**, *9*, 5056−5070.
(25) *Schott Optical Glass Catalog*; Mainz, Germany, 2004.
(26) *Release on the Refractive Index of Ordinary Water Substance as a Function of Wavelength, Temperature and Pressure*; Steam International Association for the Properties of Water and Steam: Erlangen, Germany, 1997; pp 2−3.
(27) *CRC Handbok of Chemistry and Physics, Internet Version*; Taylor and Francis: Boca Raton, FL, 2006.

mass per unit area using[18]

$$\Gamma = \frac{\mathrm{d}(n - n_{\mathrm{bulk}})}{\mathrm{d}n/\mathrm{d}c} \quad (1)$$

where n_{bulk} is the refractive index of the bulk aqueous solution, and $\mathrm{d}n/\mathrm{d}c$ is the refractive index increment of PDMAEMA in water, 0.18 cm^3/g.[28] Although regressed values of n and d are highly coupled and their values are based on the assumed model of a homogeneous film structure, their errors are mutually compensating and the surface concentration calculated from them is valid and model-independent.[29] It should be noted that the addition of a thin dielectric layer on top of the Cr/Au film shifts the position of the resonance angle (i.e., the angle of minimum reflectivity) but not the value of the reflectivity at the minimum. The latter is fixed by the Cr/Au film thickness, so it is straightforward to distinguish the optical properties of the metallic and dielectric films. The grafting density σ of the polymer layer (number of chains per unit surface area) was approximated by dividing Γ by the SEC-measured PDMAEMA molecular weight.

After protein uptake by the covalently grafted PDMAEMA layer, a new reflectivity vs angle scan was recorded. For analysis, the protein was assumed to be mixed homogeneously with the PDMAEMA layer. Thus a new optical average refractive index and thickness of the mixed PDMAEMA/protein layer were determined by data regression and the protein surface excess concentration was determined by[29]

$$\Gamma_2 = \frac{\mathrm{d}_{\mathrm{mixed}}(n_{\mathrm{mixed}} - n_{\mathrm{bulk}}) - \Gamma_1\left(\frac{\mathrm{d}n}{\mathrm{d}c}\right)_1}{\left(\frac{\mathrm{d}n}{\mathrm{d}c}\right)_2} \quad (2)$$

Subscript 1 refers to the covalently grafted PDMAEMA and subscript 2 to protein. Γ_1 was fixed at the value measured prior to protein uptake. Equation 2 states that the change in the quantity $\mathrm{d}(n - n_{\mathrm{bulk}})$ is caused by the addition of protein to the previously characterized PDMAEMA film. The refractive index increments for BSA and for lysozyme are also 0.18 cm^3/g.[30] We note that similar protein uptake values are obtained whether we use this mixed film model or treat the bound protein as a separate film on top of a distinct PDMAEMA layer. This confirms that the mass concentration determined from SPR does not depend on the details of the optical model used to describe the interface, similar to ellipsometry and optical reflectometry.

Results and Discussion

BSA Uptake by PDMAEMA Layers. Figure 2 shows representative SPR data and regressions for a bare gold surface immersed in 1 mM NaCl, the same surface after growing PDMAEMA (MW 100 000) and finally after BSA uptake into that PDMAEMA layer from a 0.1 mg/mL solution. Although the Fresnel multilayer model predicts that any dielectric adlayers with refractive index larger than that of the bulk solution will shift the SPR profile to higher incident angle without changing the reflectivity value at the resonance angle (the minimum reflectivity), we frequently observed a slight decrease in the minimum reflectivity after grafting the PDMAEMA layer from the gold surface. We believe this is due to a small loss of gold during the polymerization. This required a small adjustment to the gold film thickness (typically 2% or less, while holding d_{Cr}, n_{Cr}, and n_{Au} constant) to match the minimum reflectivity.

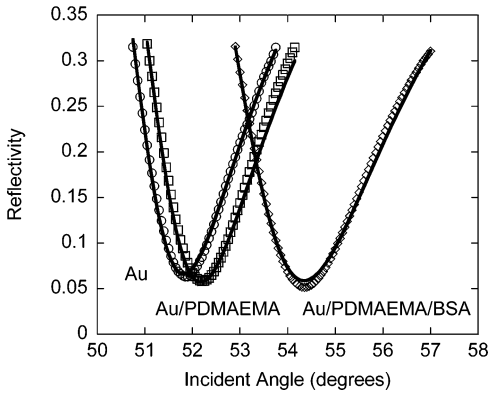

Figure 2. Representative SPR curves all measured in the presence of 1 mM NaCl solution and the corresponding fits for a bare gold surface (Au, circles), the same gold surface with grafted PDMAEMA (Au/PDMAEMA, squares) and after BSA adsorption on the same grafted PDMAEMA layer (Au/PDMAEMA/BSA, diamonds). Temperature was maintained at 25 °C. Curve Au was fitted with four-layer model ($d_{\mathrm{Cr}} = 0.6$ nm, $n_{\mathrm{Au}} = 0.32 + 3.43\mathrm{i}$, and $d_{\mathrm{Au}} = 47.8$ nm). All of these parameters were used in the five-layer model employed for fitting curve Au/PDMAEMA and curve Au/PDMAEMA/BSA to quantify the surface excess concentrations $\Gamma_{\mathrm{PDMAEMA}}$ and Γ_{BSA}, but d_{Au} was adjusted to 47.2 nm to match the minimum reflectivity of curve Au/PDMAEMA. $\Gamma_{\mathrm{PDMAEMA}} = 5.1$ mg/m^2, calculated from the fitted parameters $n_{\mathrm{film}} = 1.339$, $d_{\mathrm{film}} = 130$ nm after grafting. After BSA adsorption, $n_{\mathrm{film}} = 1.480$, $d_{\mathrm{film}} = 26$ nm, giving $\Gamma_{\mathrm{BSA}} = 16.3$ mg/m^2.

The SPR profile for the grafted PDMAEMA layer was regressed with $n_{\mathrm{film}} = 1.339$ and $d_{\mathrm{film}} = 130$ nm, corresponding to a surface excess concentration of $\Gamma_{\mathrm{PDMAEMA}} = 5.1$ mg/m^2 ($\sigma^{-1} = 33$ nm^2 per chain). Injecting 3 mL of thermally equilibrated BSA solution (0.1 mg/mL in 1 mM NaCl, pH 5.8) through the SPR flowcell (41 flowcell volumes) dramatically shifted the SPR profile to higher incident angles. This is indicative of a very large amount of BSA adsorption. The resulting mixed film profile was regressed with $\mathrm{d}_{\mathrm{mixed}}(n_{\mathrm{mixed}} - n_{\mathrm{bulk}}) = 3.85$ nm, corresponding to a surface excess concentration of BSA, $\Gamma_{\mathrm{BSA}} = 16.3$ mg/m^2, calculated from eq 2. We emphasize that the surface excess concentrations are the physically significant products of this analytical procedure, more so than the individually regressed values of index and thickness whose values are highly coupled. No detectable BSA loss occurred when the surface was rinsed with 1 mM NaCl.

For comparison, we used SPR to measure BSA adsorption to hydrophobic self-assembled monolayers (SAMs) of hexadecanethiol on gold. The SAMs were prepared according to well-established procedures.[31] BSA was allowed to adsorb to the SAM from a 0.1 mg/mL solution in 1 mM NaCl. The BSA surface concentration reached 2.0 mg/m^2 after 20 h and 3.1 mg/m^2 after 115 h. This extent of adsorption is consistent with a monolayer of BSA molecules (represented as a 3 nm thick equilateral triangle measuring 8 nm on a side[32] and having molecular weight 66 kD[33]). Both this extent of BSA adsorption on hydrophobic surfaces and the prolonged adsorption over many hours are consistent with measurements made using techniques other than SPR (reflectometry,[34] radiolabeling,[35] and ellipsometry[36,37]). Thus,

(28) Theodoly, O.; Cascão-Pereira, L.; Bergeron, V.; Radke, C. J. *Langmuir* **2005**, *21*, 10127−10139.
(29) Tilton, R. D. Scanning Angle Reflectomery and Its Application to Polymer Adsorption and Coadsorption with Surfactants. In *Colloid-Polymer Interactions: From Fundamentals to Practice*; Farinato, R. S., Dubin, P. L., Eds.; John Wiley & Sons: New York, 1999; pp 331−363.
(30) Robeson, J. L.; Tilton, R. D. *Langmuir* **1996**, *12*, 6104−6113.
(31) Hou, Z.; Dante, S.; Abbott, N. L.; Stroeve, P. *Langmuir* **1999**, *15*, 3011−3014.
(32) Carter, D. C.; Ho, J. X. *Adv. Protein Chem.* **1994**, *45*, 153−203.
(33) Hirayama, K.; Akashi, S.; Furuya, M.; Fukuhara, K. *Biochem. Biophys. Res. Commun.* **1990**, *173*, 639−646.
(34) Butler, S. M.; Tracy, M. A.; Tilton, R. D. *J. Controlled Release* **1999**, *58*, 335−347.
(35) Lee, S. H.; Ruckenstein, E. *J. Colloid Interface Sci.* **1988**, *125*, 365−379.
(36) Giacomelli, C. E.; Esplandiú, M. J.; Ortiz, P. I.; Avena, M. J.; De Pauli, C. P. *J. Colloid Interface Sci.* **1999**, *218*, 404−411.

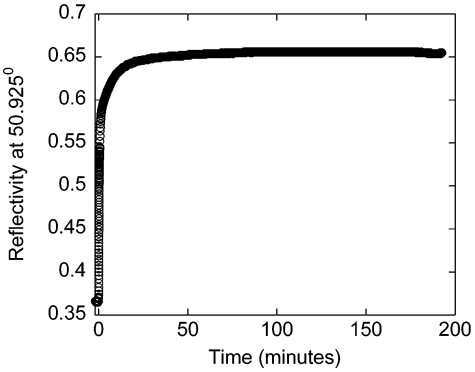

Figure 3. Kinetics of BSA uptake by a PDMAEMA brush from a 0.1 mg/mL BSA solution in 1 mM NaCl as indicated by the changing reflectivity at a fixed incident angle of 50.925°. A total of 3 mL of solution were passed through the flowcell by manual injection over the first 20 s of the measurement. The solution was stagnant thereafter.

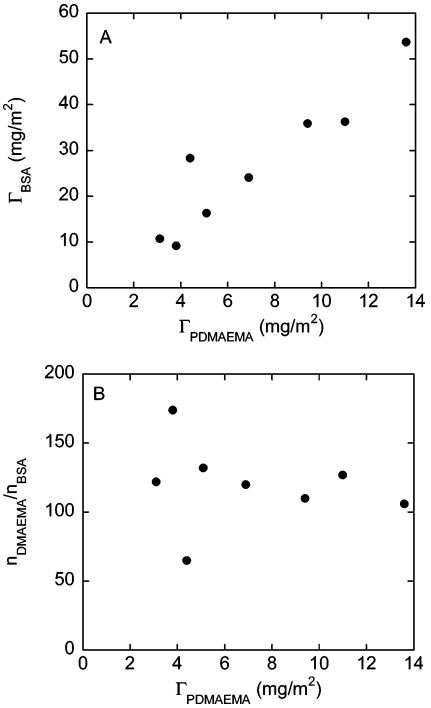

Figure 4. BSA surface excess concentrations scale linearly with the PDMAEMA surface concentration (A), indicating a constant average number of DMAEMA monomers per bound BSA molecule plotted as n_{DMAEMA}/n_{BSA} in (B).

the extent of BSA uptake in the grafted PDMAEMA layer in Figure 2 is equivalent to ~5 monolayers of BSA. As shown in Figure 3, BSA uptake in PDMAEMA layers reached completion in ~2 h, far less time than is required for BSA adsorption onto a flat hydrophobic surface.

The extent of BSA adsorption on different PDMAEMA layers (prepared with different grafting densities and M_n ranging from 12 000−100 000) is summarized in Table 1 and plotted in Figure 4. The BSA concentration was 0.1 mg/mL in 1 mM NaCl solutions in all experiments. The pH of these BSA solutions was 5.8. The surface concentration of grafted PDMAEMA used in these experiments ranged from 3.1 to 13.6 mg/m^2, with σ^{-1} ranging from 2 to 54 nm^2 per chain. It is apparent that the PDMAEMA layers take up BSA to a greater extent than can be accommodated in an adsorbed monolayer, over the entire range of PDMAEMA layer coverages examined.

High extents of BSA adsorption have been reported previously, albeit under extreme conditions. Asanov[38] reported $\Gamma_{BSA} = 8-50$ mg/m^2 on quartz surfaces at pH 6.2 when ammonium sulfate was added at high concentrations. The high adsorption was due to salting out. Such is not the case here.

The pK_a for PDMAEMA in solution is 7.5,[39] and the isolectric point for BSA is ~4.7. At pH 5.8, BSA would have a net electrostatic attraction to the cationic amine groups of the PDMAEMA layers. The large BSA uptake is likely due to the electrostatically driven penetration of the positively charged PDMAEMA layer.

Figure 4 shows that the extent of BSA uptake scales linearly with the surface concentration of PDMAEMA, indicating that the average number of DMAEMA monomers per bound BSA molecule is a constant. Averaging over all the samples examined gives $n_{DMAEMA}/n_{BSA} = 120 \pm 30$ at saturation.

Brush Conditions. The extension of an end-grafted polymer layer is determined by the dimensionless separation distance between chains, calculated as $2R_g\sigma^{1/2}$, where R_g is the radius of gyration that a free chain would have in solution. The grafted layer forms a brush when $2R_g\sigma^{1/2} > 1$, as the strong interchain interactions require chain stretching. PDMAEMA in solution can be approximated by a Gaussian density profile such that $R_g = (Na^2/6)^{1/2}$, where Na must equal the contour length ($Na = 0.25$ nm·n_{DMAEMA}) and a is the statistical segment length.[40] The degree of polymerization n_{DMAEMA} is obtained simply by dividing the number-average molecular weight M_n by the molecular weight of the DMAEMA monomer. Small-angle neutron scattering from aqueous PDMAEMA solutions shows that $a = a_0\alpha^{0.2}$ where $a_0 = 1.54$ nm and α is the degree of protonation of the polymer.[40] At pH 5.8, using a pK_a of 7.5,[39] we estimate $\alpha = ([H^+]/K_a)/(1 + [H^+]/K_a)$ to be 0.98.

Values of the dimensionless separation distance $2R_g\sigma^{1/2}$, listed in Table 1, exceeded one for all samples. All of the PDMAEMA layers were therefore judged to be brushes. The suggested picture of BSA imbibed amidst the grafted PDMAEMA brush allows one to estimate the equivalent three-dimensional concentration of BSA within the layer as $C_{3D,BSA} = \Gamma_{BSA}/H$, provided the layer thickness H can be estimated.

It should be noted that SPR is not able to resolve the details of the BSA distribution within the PDMAEMA brush, nor can it quantitatively reveal the effect of BSA uptake on the brush layer thickness, so we choose to use theoretical models of brush thickness in order to estimate three-dimensional BSA concentrations. The mean-field theory developed by Zhulina[41] predicts that the thickness of an annealed polyelectrolyte brush in the osmotic regime (low electrolyte concentration) is $H \cong Na\alpha^{1/2}$. To illustrate, sample 4 for which $M_n = 80\,000$ is expected to have $H = 126$ nm and the surface concentration $\Gamma_{BSA} = 53.7$ mg/m^2 would correspond to $C_{3D,BSA} = 426$ mg/mL. This is approximately 80% of the solubility limit of BSA in water (535 mg/mL).[42]

Figure 5 shows that over all of the samples examined, the apparent three-dimensional protein concentration in the PDMAEMA layer varies from 58 to 1897 mg/mL. This is the binding

(37) McClellan, S. J.; Franses, E. I. *Colloids Surf. A* **2005**, *260*, 265−275.
(38) Asanov, A. N.; DeLucas, L. J.; Oldham, P. B.; Wilson, W. W. *J. Colloid Interface Sci.* **1997**, *196*, 62−73.
(39) van de Wetering, P.; Moret, E. E.; Schuurmans-Nieuwenbroek, N. M. E.; van Steenbergen, M. J.; Hennink, W. E. *Bioconjugate Chem.* **1999**, *10*, 589−597.
(40) Lee, A. S.; Bütün, V.; Vamvakaki, M.; Armes, S. P.; Pople, J. A.; Gast, A. P. *Macromolecules* **2002**, *35*, 8540−8551.
(41) Zhulina, E. B.; Birshtein, T. M.; Borisov, O. V. *Macromolecules* **1995**, *28*, 1491−1499.
(42) Kozinski, A. A.; Lightfoot, E. N. *AIChE J.* **1972**, *18*, 1030−1040.

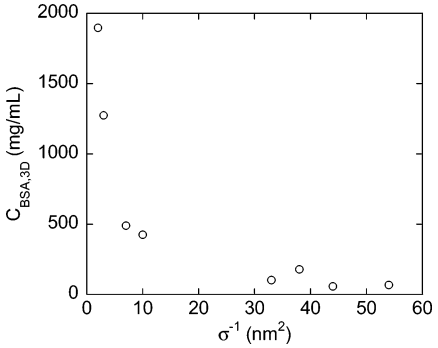

Figure 5. Equivalent three-dimensional concentration of BSA as a function of surface area per PDMAEMA chain.

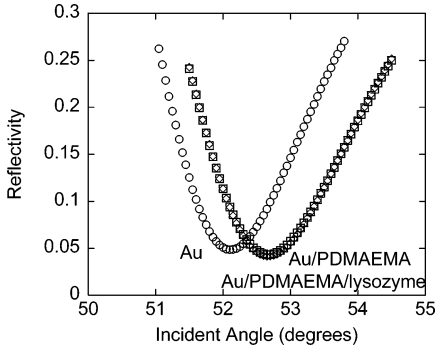

Figure 6. Representative SPR profiles for the bare gold surface immersed in 1 mM NaCl at 25 °C (Au, circles), the gold surface after PDMAEMA grafting (Au/PDMAEMA, squares) and after incubation of the PDMAEMA layer with 0.1 mg/mL lysozyme in 1 mM NaCl for 24 h (Au/PDMAEMA/lysozyme, diamonds). The latter two profiles are superimposed indicating the absence of lysozyme adsorption.

capacity of the brush, and it decreases monotonically with increasing surface area per PDMAEMA chain. This suggests that BSA is directly attached to PDMAEMA segments following the ratio 120 DMAEMA monomers per BSA calculated previously; BSA is not driven to fill any "interstitial" three-dimensional space that remains available between PDMAEMA chains which is occupied by solvent molecules. Although each grafted PDMAEMA chain binds BSA molecules directly, increasing the space between those grafted chains has the effect of decreasing the overall density of BSA in the film. The picture that emerges is of individual chains decorated with BSA molecules, where increasing or decreasing the interchain spacing has little effect on the number of proteins bound per chain. We emphasize that these three-dimensional concentrations are estimates, based on a model for the thickness of end-grafted polyelectrolyte brushes in the absence of bound proteins.

The suggested penetration of BSA throughout the brushes that emerges from our analysis is similar to observations reported by Hunter and Carta regarding protein uptake in acrylamido-based anion-exchanger gels.[43] Hunter and Carta argued that favorable electrostatic interactions between the protein and the gel would overcome the size exclusion effect, provided that the size of the protein was not too large relative to the pore size. For high ionic strengths where electrostatic attractions were screened, they found that size exclusion effects became more important. A recent study by Yoshikawa and co-workers showed that the size exclusion effect controls protein adsorption on grafted neutral hydrophilic polymer layers.[44] Thus, protein uptake into a polymer brush requires a strong protein attraction to the polymer.

The binding capacity of PDMAEMA brushes for BSA is put into perspective by considering binding capacities for other ion exchange media.[1,8,45−49] The protein binding capacity of grafted PDMAEMA layers at high grafting densities is comparable to the highest reported static binding capacity value of 400 mg/mL reported by Lewus and Carta[8] for the absorption of cytochrome *c* into anionic polyacrylamide-based hydrogels.

Electrostatic Selectivity. To compare with the high capacity uptake of BSA, PDMAEMA brushes were also exposed to 0.1 mg/mL solutions of lysozyme in 1 mM NaCl. These solutions were pH 5.7. Having an isoelectric point of pH 11, chicken egg lysozyme carries a net positive charge at pH 5.7. As shown in Figure 6, lysozyme adsorbed negligibly to the PDMAEMA brush. There was no distinguishable shift in the SPR reflectivity profile after 24 h of lysozyme exposure to the brush. The complete rejection of lysozyme by grafted PDMAEMA layers is due to the electrostatic repulsion between the two entities.

Complete rejection of proteins having the same net charge as the polyelectrolyte is not always observed in the literature. Net negatively charged fibrinogen adsorbed considerably on poly(styrenesulfonic acid) brushes,[6] as did negatively charged BSA on poly(acrylic acid).[7] The ability to bind a protein against a net electrostatic repulsion may arise from locally favorable interactions with oppositely charged patches on the protein surface. Entropy changes in proteins with relatively low conformational stability may also help drive adsorption against a net electrostatic repulsion.[50] The inability of lysozyme to be taken up at all by PDMAEMA may reflect its relatively small size and its high degree of conformational stability.

Desorption of BSA from PDMAEMA Brushes. Although the results presented above indicate that PDMAEMA brushes have a high protein binding capacity and charge selectivity, it must be possible to remove the bound protein from the brush if these brushes are to be useful as ion exchange media. As noted above, merely rinsing the BSA-laden brush with a BSA-free 1 mM NaCl solution caused no significant desorption. Here we examine the effects of pH and ionic strength on desorption during rinsing.

We first considered BSA desorption at pH 4, slightly below the BSA isoelectric point, where BSA and PDMAEMA will have a (weak) net electrostatic repulsion. Figure 7 shows the SPR profiles from a representative experiment. BSA was adsorbed at pH 5.8 in the presence of 1 mM NaCl as above. The first rinse was performed with a 1 mM NaCl solution that had been acidified to pH 4 by adding HCl. This solution was pumped past the surface at 1 mL/min for 6 h and caused the SPR profile to shift back almost to the pre-BSA adsorption profile. 83% of the adsorbed BSA was removed from the brush by this rinsing step (Γ_{BSA} decreased from 28.3 mg/m^2 to 4.7 mg/m^2). Subsequently, additional removal up to 87% was achieved by flowing a pH 4, 1 M NaCl solution over the surface for 1 h ($\Gamma_{BSA} = 3.6$ mg/m^2).

At pH 4, not very far from the isoelectric point of BSA, localized electrostatic attraction between PDMAEMA chains and nega-

(43) Hunter, A. K.; Carta, G. *J. Chromatogr. A* **2002**, *971*, 105−116.
(44) Yoshikawa, C.; Goto, A.; Tsujii, Y.; Fukuda, T.; Kimura, T.; Yamamoto, K.; Kishida, A. *Macromolecules* **2006**, *39*, 2284−2290.
(45) Hunter, A. K.; Carta, G. *J. Chromatogr. A* **2000**, *897*, 65−80.
(46) Boschetti, E. *J. Chromatogr. A* **1994**, *658*, 207−236.
(47) Staby, A.; Sand, M.; Hansen, R. G.; Jacobsen, J. H.; Andersen, L. A.; Gerstenberg, M.; Bruus, U. K.; Jensen, I. H. *J. Chromatogr. A* **2005**, *1069*, 65−77.
(48) Staby, A.; Sand, M.; Hansen, R. G.; Jacobsen, J. H.; Andersen, L. A.; Gerstenberg, M.; Bruus, U. K.; Jensen, I. H. *J. Chromatogr. A* **2004**, *1034*, 85−97.
(49) Lewus, R. K.; Carta, G. *AIChE J.* **1999**, *45*, 512−522.
(50) Norde, W. Driving Forces for Protein Adsorption at Solid Surfaces. In *Biopolymers at interfaces*; Malmsten, M., Ed.; Marcel Dekker: New York, 2003; pp 21−43.

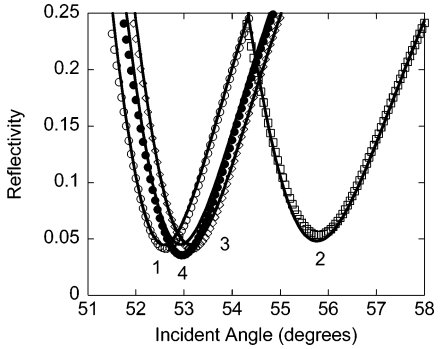

Figure 7. SPR curves and the fits of PDMAEMA-modified Au (1), after BSA adsorption (2), after pH 4, 1 mM NaCl wash (3), and after pH 4, 1M NaCl wash (4).

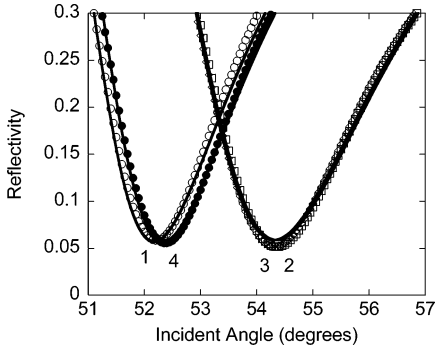

Figure 8. SPR profiles and regressions for PDMAEMA-modified Au (1), after BSA adsorption from 1 mM NaCl solution (2), after pH 9, 1 mM NaCl rinse (3), and after pH 9, 1 M NaCl rinse (4). Only a small amount of BSA desorbed after the pH 9, 1 mM rinse as indicated by the superposition of curves 2 and 3.

tively charged patches on BSA is still likely to occur. The additional desorption caused by increasing the ionic strength to 1 M NaCl may be attributed to screening localized electrostatic attractions or to competitive adsorption of Cl^- ions to displace BSA from the brush. The final residual of 3.6 mg/m^2 may indicate that although the PDMAEMA/BSA interactions are predominantly electrostatic in nature, hydrophobic interactions may also play a role. Direct BSA adsorption to regions of the solid surface between grafts is also a possibility in this experiment, where $\sigma^{-1} = 38$ nm^2/chain.

We next considered rinsing with a pH 9 solution to decrease the electrostatic attraction by neutralizing the PDMAEMA brush. At pH 9 the degree of ionization in the PDMAEMA brush should be <3%. The rinse solution was prepared with NaOH to reach pH 9. Figure 8 shows representative SPR profiles of the adsorption of BSA under the usual conditions described above, followed first by rinsing with a pH 9, 1 mM NaCl solution at a flowrate of 1 mL/min for 1 h, followed by rinsing with a pH 9, 1 M NaCl solution for 5 h. Increasing the pH to 9 while maintaining a low ionic strength caused negligible desorption (Γ_{BSA} decreased from 16.3 to 16.0 mg/m^2), but the subsequent rinse with pH 9, 1 M NaCl decreased Γ_{BSA} to 3.2 mg/m^2. Merely decreasing the degree of ionization of the PDMAEMA chains was insufficient to desorb the BSA; it was also necessary to screen the remaining electrostatic attraction. It is possible that ion pairs between acidic amino acid residues and PDMAEMA amine groups had to be disrupted by competitive binding by Na^+ and Cl^-.

Conclusions

Layers of PDMAEMA grafted from a solid surface demonstrate a high capacity for electrostatically selective protein uptake. The net negatively charged protein BSA was taken up in amounts that approach its aqueous solubility limit in the case of PDMAEMA brushes at high grafting densities. These are among the highest reported protein binding capacities for ion exchange media. BSA binding scaled linearly with the mass of PDMAEMA grafted per unit area, with a constant ratio of approximately 120 DMAEMA monomer units per bound BSA molecule. The kinetics of BSA uptake in the brush were considerably more rapid than the slow asymptotic approach to adsorption saturation that is often seen for BSA adsorption to a solid surface. The high affinity for BSA was evident in the complete lack of desorption from the brush when rinsing with dilute NaCl solutions. Desorption could be achieved by using pH and/or ionic strength changes to interfere with the electrostatic attraction for BSA. In contrast, PDMAEMA had no affinity for the net positively charged protein lysozyme. These results indicate that PDMAEMA can be a charge selective, high capacity ion exchange medium for protein binding.

Acknowledgment. This material is based on work supported by the National Science Foundation under Grant CTS-0304568.

LA063660B